Proceedings World Geothermal Congress 2026
Calgary, Canada, June 8 – 11, 2026

An Analytical Model to Calculate the Thermal Conductivity of the Reference Crab Orchard Reservoir Rocks

Maria Alejandra Taborda[1]*, Jasmin Raymond[1] and Stéphanie Larmagnat[2]
Institut national de la recherche scientifique (Québec)- INRS[1]*, Geological Survey of Canada (Québec)- GSC[2]
maria-alejandra.taborda-ortiz@inrs.ca

Keywords: Thermal conductivity, Porosity, Analytical models, Crab Orchard Sandstone

ABSTRACT

Characterizing the thermohydraulic properties of reservoirs is essential for the development of geothermal projects. Models to predict the thermal conductivity of a rock formation can be useful when direct measurements on samples cannot be made in the laboratory. The objective of this research was to evaluate the variation of thermal conductivity as a function of porosity in a reference reservoir lithology, to determine which analytical model can be used to accurately calculate its thermal conductivity. Crab Orchard Sandstone was chosen for its representative reservoir properties, making it a suitable analog for the study of sedimentary basin reservoirs. For example, Crab Orchard is used as an analog to the Cairnside and Covey Hill Formations in the St. Lawrence Lowlands sedimentary basin to study carbon dioxide storage combined with geothermal energy extraction. Measurements were carried out on nine core samples. Porosity was determined using a combined permeameter and porosimeter, and bulk thermal conductivity was measured on dry and saturated samples using an optical thermal conductivity scanner. The arithmetic, geometric and harmonic averages were then used to determine which model best reproduces the sample thermal conductivity that was evaluated with the TCS in dry and saturated conditions. The model that gave the most meaningful results was the geometric average with a maximum relative error in thermal conductivity of 5.5%. The estimated thermal conductivity of solids was 6.49 $Wm^{-1}K^{-1}$. Under a known porosity, we can now predict the Crab Orchard Sandstone thermal conductivity with an acceptable margin of error for samples with similar mineralogy.

1 INTRODUCTION

Geothermal is considered as a clean and renewable energy, generating an amount of greenhouse-gas emissions similar to hydropower, solar or other alternative energy sources (Ármannsson *et al.*, 2005; Kagel *et al.*, 2005; Umar *et al.*, 2023). The thermohydraulic properties of rocks are essential input parameters for models to simulate fluid flow and heat transfer, which is crucial for geothermal potential assessment (Abdulagatov *et al.*, 2015; Di Sipio *et al.*, 2013; Popov *et al.*, 2016; Raymond *et al.*, 2017). These properties include thermal conductivity (TC), which controls the transport and exchange of heat by conduction (Cho *et al.*, 2009; Wu *et al.*, 2023). There are categories of methods for measuring TC, working at different scales, e.g., in situ field experiments like thermal response tests, indirect measurements such as geophysical well logs and temperature profiles or diverse laboratory methods made on samples (Raymond, 2018). However, it is not always possible to implement these techniques to determine the TC, in particular at the samples scale, due to sample size limitations, the representativeness of the core intervals, the costs of analysis, or the destructive or invasive nature of certain methods (Hu *et al.*, 2025).

The Thermal Conductivity Scanner (TCS) allows measuring samples of a large range of size, and is an efficient non-destructive transient laboratory technique to characterize TC (Popov *et al.*, 2016; Popov *et al.*, 1999). There is no contact between the sensors and the sample, it has a high operating speed and short measurement time, and it effectively assesses thermal anisotropy and detects sample heterogeneity. Nevertheless, black color applied to the samples is necessary to ensure absorption of the infrared heat waves emitted during the measurement. Yet, painting may affect the results of chemical analyses, for example, the isotopic ratio of strontium due to its abundance and variations (Murphy *et al.*, 2020; Vroon *et al.*, 2008) and its impact can be significant in multidisciplinary studies.

This study objective was to evaluate variation in TC as a function of porosity in a reference reservoir lithology, specifically sandstone, to determine which analytical models (arithmetic, geometric or harmonic averages) can be used to accurately calculate its TC. Understanding these relationships is key to optimizing geothermal exploration studies. The Crab Orchard sandstone was selected for this purpose. It is one of the lithologies

offered by Kocurek Industries, a rock provider based in Texas, who specialized in supplying high-quality reservoir rock samples for academic and industrial research.

2 METHODOLOGY

Measurements were carried out at the *Laboratoire ouvert de géothermie* (LOG) of INRS. Nine rock core samples (Crab Orchard), each with a maximum length of 9.60 cm, were cut, polished, and the end faces flattened to ensure optimal surface quality. They were then dried in a conventional oven at 108°C for 48 hours prior to laboratory measurements. Porosity was measured using the grain volume system of the combined permeameter and porosimeter (AP-608 from CoreTest). Grain volume measurements were made using helium expansion based on Boyle's Law (Raymond *et al.*, 2017). TC was determined with an infrared TCS from Lippman Geophysikalische Messgeräte. TC was measured for samples both in dry and saturated conditions (using distilled water). Measurements on the saturated samples were carried out after leaving the samples immersed for 48 hours and by turning the TCS upside down. While the protocol itself was already known, we apply a custom setup developed through internal experience and practice at the LOG, as shown in Figure 1.



Figure 1a. Method to determine thermal properties for regular dry samples (TCS is used in its conventional operating position).

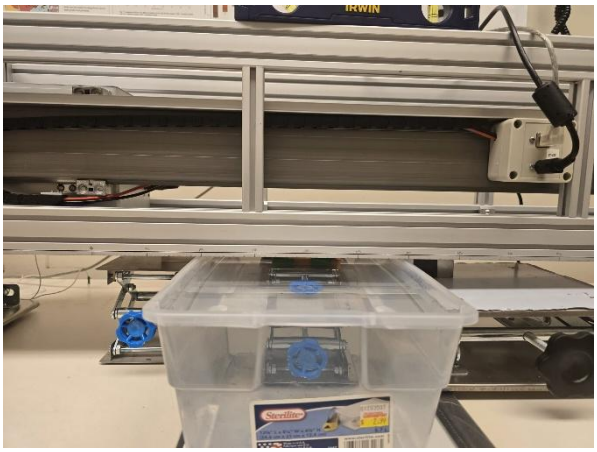


Figure 1b. Method to determine thermal properties in saturated samples (TCS is used here in an upside-down position).

TC of the solid phase was then calculated using arithmetic, geometric, and harmonic means according to the formulations in Clauser (2014), and based on the bulk thermal conductivity (λ_b) values obtained from dry and saturated samples (Equations 1, 2 and 3):

$$\lambda_{b-arit.} = (1-\theta)\lambda_s + \theta\lambda_f \quad (1)$$

$$\lambda_{b-geo.} = \lambda_s^{(1-\theta)} \times \lambda_f^{\theta} \quad (2)$$

$$\lambda_{b-har.} = \left(\left[\frac{(1-\theta)}{\lambda_s}\right] + \left[\frac{\theta}{\lambda_f}\right]\right)^{-1} \quad (3)$$

where λ_s and λ_f (W m^{-1} K^{-1}) corresponds to TC of the solids and fluid and θ (%) is the measured porosity. Air and water TC use in the subsequent calculations are assumed equal to 0.026 W m^{-1} K^{-1} and 0.6 W m^{-1} K^{-1}, respectively (Kappelmeyer & Haenel, 1974).

After calculating the λ_s using the above equations for both dry and water saturated conditions with the three models, the model with the smallest difference was determined, since the λ_s is expected to be the same for all conditions. Then, considering the range between the lowest and highest of 18 results (9 values were obtained from dry samples and 9 from saturated samples), the λ_s with the most optimal value was selected. This optimal value was obtained with the average of the lower root mean squared error (RMSE) calculated for both dry λ_b and saturated λ_b (Equation 4):

$$\text{RMSE} = \frac{1}{n}\sum(\lambda_{b-calculated} - \lambda_{b-measured})^2 \quad (4)$$

where n is the total number of observations (9), $\lambda_{b\ calculated}$ is the TC obtained through the model and $\lambda_{b\ measured}$ is the TC measured with TCS.

Finally, the relative error was calculated based on the λ_b obtained with the optimal λ_b value found previously (Equations 1-3) and the TC values measured under both dry and water-saturated conditions (Equation 5).

$$E = \frac{|\lambda_{b-calculated} - \lambda_{b-measured}|}{\lambda_{b-measured}} \times 100 \quad (5)$$

where E (%) is the relative error.

To validate the applicability of this model, the mineral content was evaluated. Bulk materials and clay fractions from samples were analyzed by X-ray powder diffraction on a Bruker D8 Advance. Bulk samples were micronized, dried and back pressed to produce oriented powders and clays were dispersed to produce oriented mounts. Patterns were collected on a Bruker D8 Advance Powder Diffractometer (Lynx-Eye Detector, Co Kα, 35 kV, 40 mA). Samples were also X-rayed after ethylene glycol saturation and after heating to 550 °C. Minerals were identified using the EVA software and quantitative analysis was then performed using TOPAS, a PC-based program that performs Rietveld refinement of X-ray diffraction spectra (Rietveld, 1967) and is based on a whole pattern fitting algorithm with reference minerals.

3 RESULTS

Mineralogical, porosity and TC results are presented in Table 1. All Crab Orchard sandstones are predominately composed of quartz (> 95%) with minor constituents including potassic feldspar and traces amounts of plagioclase and pyrite. The mean porosity value is 9.6%, varying between 6.5% and 11.5%.

Table 1. Mineralogical composition, porosity and bulk thermal conductivity for both dry and water saturated conditions. *Qtz: quartz, Kfs: K-feldspar, Pl: plagioclase, Ms: muscovite, Kln: kaolinite.

Sample	Mineral content* (%)					Porosity (%)	λ_b dry (W m^{-1} K^{-1})	λ_b saturated (W m^{-1} K^{-1})
	Qtz	Kfs	Pl	Ms	Kln			
TS1	99	1	0	0	0	9.2	3.70	5.13
TS2	99	1	0	0	0	9.4	3.77	5.26
TS3	99	1	0	0	0	8.9	3.82	5.20
TS4	99	1	0	0	0	11.4	3.52	5.15
TS5	98	2	0	0	0	11.3	3.49	5.01
TS6	98	2	0	0	0	11.4	3.48	5.05
TS7	97	2	1	0	0	11.1	3.59	4.96
TS8	97	2	1	0	0	11.5	3.56	5.18
TS9	98	2	0	0	0	11.1	3.55	4.95
TS10	95	1	0	2	2	6.8	2.93	4.99
TS11	96	1	0	2	1	7.0	3.01	4.80
TS12	96	1	0	2	1	6.5	3.22	4.95

Models were used to determine the λ_s based on the measured λ_b determined under both dry and saturated conditions (Table 2). The model that produced the smallest difference in calculated λ_s between dry and saturated conditions was the geometric model.

A high quartz content can minimize the effect of natural rock heterogeneity on rock TC (Williams & French, 2024). This may explain the discrepancy observed in samples with a low quartz content. An attempt was made to apply the same models to samples TS10 to 12 having a quartz content of 95-96% but, because of the greater variability in accessory minerals (K-feldspar, muscovite, kaolinite, dolomite, and traces amounts of pyrite), which

influenced the λ_s and increased the error, these samples were not considered in the final calculation of the mean λ_s.

Table 2. Solids thermal conductivity from arithmetic, geometric and harmonic models.

Sample	Dry			Saturated			Difference		
	λ_s (W m^{-1} K^{-1})			λ_s (W m^{-1} K^{-1})			λ_s (W m^{-1} K^{-1})		
	Arit.	Geo.	Harm.	Arit.	Geo.	Harm.	Arit.	Geo.	Harm.
TS1	4.08	6.12	-0.28	5.59	6.38	21.79	1.52	0.26	-22.07
TS2	4.16	6.31	-0.27	5.74	6.59	26.80	1.59	0.28	-27.07
TS3	4.19	6.23	-0.29	5.65	6.42	20.87	1.46	0.19	-21.16
TS4	3.96	6.61	-0.22	5.73	6.79	210.21	1.77	0.18	-210.43
TS5	3.93	6.51	-0.22	5.57	6.56	76.46	1.64	0.06	-76.68
TS6	3.93	6.54	-0.22	5.62	6.64	106.64	1.69	0.10	-106.86
TS7	4.04	6.66	-0.22	5.51	6.46	55.66	1.47	-0.20	-55.89
TS8	4.02	6.75	-0.21	5.78	6.86	902.78	1.76	0.11	-902.99
TS9	3.99	6.56	-0.22	5.50	6.45	52.13	1.51	-0.11	-52.36
TS10	3.14	4.13	-0.41	5.31	5.83	10.73	2.18	1.70	-11.14
TS11	3.24	4.31	-0.39	5.12	5.61	10.14	1.88	1.31	-10.53
TS12	3.44	4.50	-0.43	5.26	5.74	10.04	1.82	1.24	-10.46

The geometric mean yielded the most meaningful values, in agreement with previous studies (Chopra *et al.*, 2018; Clauser, 2014; Fuchs *et al.*, 2013; Song *et al.*, 2023). The average λ_s obtained with samples TS1 to TS9 using geometric model is 6.52 W m^{-1} K^{-1}. Due to the high quartz content, the λ_s is relatively high, which in turn increases thermal conductivity of bulk rock (Suft *et al.*, 2025). However, it is important to keep in mind that the mineralogical composition of the Crab Orchard samples may vary and the quartz composition may decrease up to 85% (Benson *et al.*, 2003). Therefore, a detailed mineralogical analysis is recommended prior to applying the geometric mean model to estimate the thermal conductivity of a rock sample. For this model to be representative, the quartz content should exceed 97%.

The negative and improbable thermal conductivity values obtained with the harmonic model can be explained by the fact that the ratio of the TC of the fluid (water) to porosity is greater than the λ_b. Similar negative values have also been reported in the literature (Albert *et al.*, 2017; Fuchs *et al.*, 2013).

Considering that the geometric model showed the least variability, λ_s values ranging from 6.12 W m^{-1} K^{-1} (minimum) to 6.86 W m^{-1} K^{-1} (maximum) were used to calculate the RMSE for λ_b. The lowest RMSE values were 0.016 and 0.043, corresponding to λ_s values of 6.42 W m^{-1} K^{-1} and 6.56 W m^{-1} K^{-1} under dry and saturated conditions, respectively. The average of these λ_s values is 6.49 W m^{-1} K^{-1}.

A λ_s value of 6.49 W m^{-1} K^{-1} was then used to calculate the error in bulk thermal conductivity. The relative errors range from 0.2% to 5.5% under dry conditions and from 0.4% to 4.8% under saturated conditions, indicating that the maximum error of the geometric analytical model is 5.5%. The measured and calculated bulk thermal conductivity as a function of porosity for both dry and saturated conditions is shown in Figure 2, including 3% error bars from the TCS (Fuchs & Förster, 2014; Popov *et al.*, 1999).

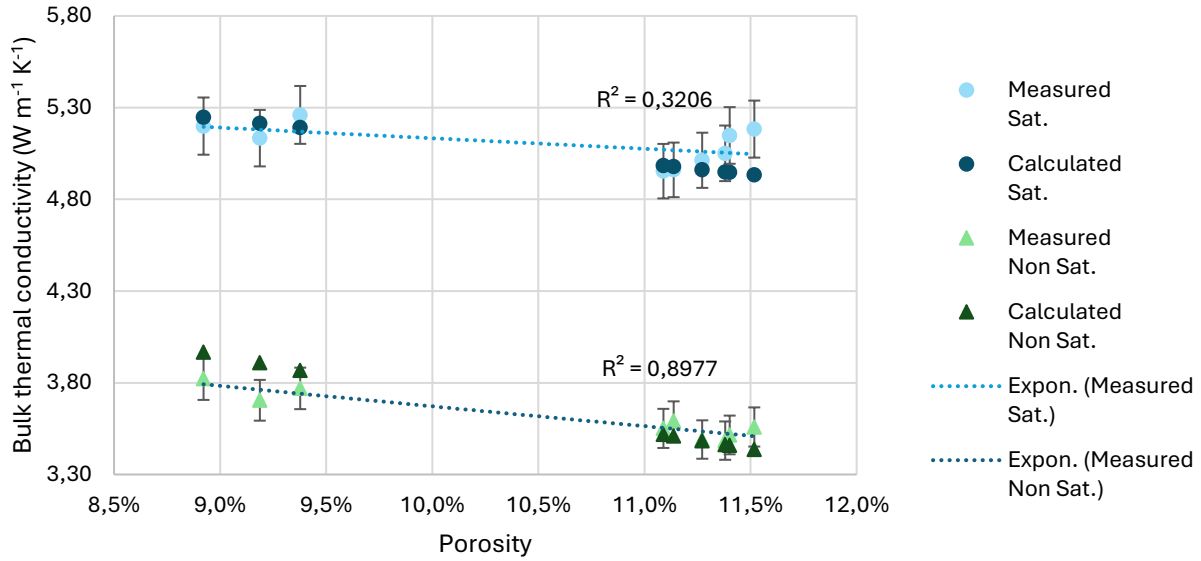


Figure 2. Measured and calculated bulk thermal conductivity considering the geometric average.

4 DISCUSSION

The TC of sandstones can range from 0.5 W m^{-1} K^{-1} to 6 W m^{-1} K^{-1} and depends on mineral composition (both matrix and grains), grain size, porosity, confining pressure, temperature, and degree of saturation (Suft *et al.*, 2025; Vivas *et al.*, 2023). To date, no TC studies have been conducted specifically on Crab Orchard sandstone. This rock unit is fine-grained and cross-bedded, with sub-hedral to sub-rounded grains. The texture is moderately well sorted and grain sizes range for 0.14 mm to 0.25 mm (Ibemesi & Benson, 2022; Velcin, 2022).

This study is part of a broader research initiative aimed at assessing the geothermal potential of the Cairnside and Covey Hill formations in the Bécancour area. In this context, the Crab Orchard sandstone was selected due to its analogy with the Cairnside and Covey Hill formations in terms of porosity and quartz content, both of which also influence TC. The results obtained here can be compared with previously reported TC values for the Cairnside and Covey Hill formations in the St. Lawrence Lowlands Sedimentary Basin, which are 6.19 ± 0.60 W m^{-1} $K^{-1}$and 4.78 ± 1.22 W m^{-1} K^{-1}, respectively (Bédard *et al.* (2017).The relatively high TC of Crab Orchard sandstone may be attributed to the well-connected network of grains, as smoother grain shapes enhance the surface contact between grains and thus heat transfer (Vivas *et al.*, 2023).

Beyond TC, porosity is an important parameter because it governs fluid circulation and storage. Previous studies on Crab Orchard sandstone report values of 5% using water porosity tests (Benson *et al.*, 2003), 5.26% using bulk and grain density measurements (Nehler *et al.*, 2019) and 10% using a helium gas porosimeter (Gehne & Benson, 2017). The average porosity of 9.6% determined in this study is closer to the latter value and to the 7-9% range indicated by the rock provider (Kocurek Industries, 2023). Moreover, each core available for this study was cut into three subsamples. Porosity among subsamples showed a maximum standard deviation of 0.23%, indicating good reproducibility with the grain volume chamber.

Because porosity directly influence fluid saturation, it is important to examine how TC changes between dry and saturated conditions. The TC of saturated samples increases in contrast to dry samples (Guo *et al.*, 2020; Mielke *et al.*, 2017). The increase is because the TC of water exceeds that of air (Nagaraju & Roy, 2014). In comparison to the study conducted by Ye *et al.* (2022), no direct proportional relationship was observed in our study between the porosity and the difference between the TC values under saturated and dry conditions (λ_b sat- λ_b dry). This difference is likely due to the limited porosity range of our Crab Orchard samples, whereas Ye *et al.* (2022) reported a broader porosity range (from 1.92% to 7.18%). Consequently, the greater porosity in our samples may explain the larger difference in conductivity between the two conditions. In any case, porosity remains a key control on TC in sedimentary rocks, which is also influenced by the type and amount of cementation (Mielke *et al.*, 2017).

Given that both TC and porosity are influenced by mineralogy, analyzing the mineral composition of Crab Orchard provides important insights. Mineral content has a significant impact on TC as individual minerals differ in their ability to conduct heat (Brigaud & Vasseur, 1989; Song *et al.*, 2023; Tang *et al.*, 2021). Rocks with high quartz content, especially when water-saturated are good heat conductors (Labus & Labus, 2018). In the present

study, samples TS10-12 were discarded. Although these samples had a high quartz content, they also contained clay minerals, which can affect TC. T he presence of clay may also explain why the geometric mean calculation for TS10–TS12 was less accurate than for samples TS1–TS9 (Albert *et al.*, 2017; Jorand *et al.*, 2011; Labus & Labus, 2018). Additional factors that may account for discrepancies in samples with a margin of error greater than 30% include the heterogeneous distribution of quartz grains of varying sizes within the sample, as well as variations in pore size and distribution (Jorand *et al.*, 2015; Song *et al.*, 2023; Tang *et al.*, 2021).

Although the geometric model may sometimes provide unrealistic results because it does not consider clay content, capillary pores and the influence of fluid saturation (Jorand *et al.*, 2011; Tatar *et al.*, 2021), it remains the model that best predict the TC of the Crab Orchard lithology. Furthermore, the effect of water saturation may be linked to the sample saturation process and the pore geometry and connectivity (Nagaraju & Roy, 2014). Despite most studies where TC was measured involved water saturation under vacuum conditions (Brigaud & Vasseur, 1989; Nagaraju & Roy, 2014; Ye *et al.*, 2022), there are previous studies where the saturation process was made at ambient temperature and pressure (Fuchs *et al.*, 2013; Jorand *et al.*, 2011) as done in the present study. Because this method does not guarantee complete saturation, it should be noted that a partial saturation may affect rock TC measurements (Nagaraju & Roy, 2014). To better understand the effect of the fluid on the TC of Crab Orchard saturated samples, future works should determine the thermal properties of the saturating fluid, in this case distilled water, and investigate the behavior of the rock under different saturation scenarios (vacuum condition, ambient temperature and pressure, and varying saturation periods). This would help clarify the role of saturation in TC variability and help improve the model. For example, in the civil engineering domain, Côté and Konrad (2005) studied the effect of fluid saturation on the thermal conductivity of soil samples, considering their degree of saturation and the temperature of the fluid under frozen and unfrozen conditions. Their approach integrates factors such as porosity, mineral content, grain-size distribution, particle shape and was validated on more than 650 tests. To determine the thermal conductivity of the samples, they applied the geometric model, which provides satisfactory results for saturated samples. The success of this model in a related domain confirms its validity and supports our methodology with results that align well with geometric average estimates.

The objective of this study was to predict the bulk thermal conductivity of any Crab Orchard sample without running lab measurements but instead using $\lambda_{s,}$ theoretical, λ_f and porosity. λ_s cannot be directly measured and was obtained from models under different conditions (Tab. 2). Different values were obtained even though λ_s would ideally be similar. This can introduce uncertainty when calculating the λ_b using the geometric average, as it assumes that the matrix TC is not affected by the TC of the pore fluid (Kämmlein & Stollhofen, 2019). Albert *et al.* (2017) presented differences of λ_s of 2.5 W m^{-1} K^{-1} between measurements made under dry and saturated conditions. In our study, the average difference is 0.17 W m^{-1} K^{-1}, which is considered acceptable.

Due to the uncertainty generated by the λ_s obtained through the geometric model, it is possible to find λ_b values either higher or lower than those measured experimentally (Fuchs *et al.*, 2013; Ye *et al.*, 2022). In this study, the geometric model returned 50% of λ_b values (6 out of 12) higher than the measured values under dry conditions and 42% (5 out of 12) higher under saturated conditions. Samples with porosity below 7% (TS10–TS12) overestimated λ_b by up to 1.5 W m^{-1} K^{-1} (52.3% error) and 0.7 W m^{-1} K^{-1} (13.2% error), under dry and saturated conditions, respectively. The overestimation in dry conditions was greater than under saturated conditions (Pichugin *et al.*, 2022). However, our decision to discard results from low-porosity samples contrasts with the conclusions of Pichugin *et al.* (2022), who reported greater errors (up to 53%) in samples with higher porosity (27.6%), and those of and by Nagaraju and Roy (2014), who found that porosity values of 5–8% produced errors of up to 15%, while porosities below 5% were associated with an uncertainty of about 10%.

The low error values obtained in this study highlight the strong predictive performance of the geometric model and support its suitability for accurately representing TC of Crab Orchard sandstones. Nevertheless, these results should be interpreted considering the model's inherent limitations, which suggest that further refinement may still enhance its predictive capability under broader conditions. The error reported in this study for the difference between measured and calculated λ_b values using the geometric model ranges from 0.2% to 5.5%. This result is considered acceptable, as previous studies have reported similar or lower deviations. For instance, Tatar *et al.* (2021) found an average absolute relative deviation of 6.85%, which was classified as accurate. Similarly, Chopra *et al.* (2018) defined an uncertainty threshold of 10%, and Fuchs *et al.* (2013) reported deviations below 20%, with errors of 5% and 6%, and still regarded the results as a good fit. In contrast, Ye *et al.* (2022) reported relative errors of 19% and 21%, which were considered large.

5 CONCLUSION

Thermohydraulic measurements performed on the Crab Orchard sandstone samples provided valuable insights into the factors influencing the evaluation of bulk thermal conductivity in this reservoir rock.

The main findings of this study are as follows:

- The geometric average can be reliably used to estimate bulk thermal conductivity as a function of porosity and solid thermal conductivity for Crab Orchard sandstone, with an uncertainty below approximately 5.5%, when the quartz content exceeds 97% and porosity is greater than 8.9%. However, for detailed studies, direct measurements of thermal conductivity are always preferred over estimated values.
- The optimal value of solid thermal conductivity obtained for Crab Orchard sandstone with quartz contents above 97% and porosities between 8.9% and 11.5% is 6.49 $W\,m^{-1}\,K^{-1}$.
- Although the samples exhibited similar quartz contents, variations in measured thermal conductivity were associated with differences in porosity, grain distribution, clay content, and saturation conditions.

The results of this study support the use of the geometric model to estimate thermal conductivity in cases where direct measurements are not feasible. For instance, to evaluate potential changes in rock thermal properties resulting from interactions between CO_2, brine, and rock.

Acknowledgements

The project was mainly supported by the Research Affiliate Program of the Natural Resources of Canada and the INRS in the context of MSc thesis on rock thermal properties and geochemistry applied to geothermal energy. Measurements were done thanks to the *Laboratoire ouvert de géothermie*. Additionally, XRD mineralogical analyses were done by the Geological Survey of Canada lab in Ottawa, Ontario.

REFERENCES

Abdulagatov, I.M., Abdulagatova, Z.Z., Kallaev, S.N., Bakmaev, A.G. and Ranjith, P.G.: Thermal-Diffusivity and Heat-Capacity Measurements of Sandstone at High Temperatures Using Laser Flash and DSC Methods. *International Journal of Thermophysics* **36**, (2015), 658-691.

Albert, K., Schulze, M., Franz, C., Koenigsdorff, R. and Zosseder, K.: Thermal conductivity estimation model considering the effect of water saturation explaining the heterogeneity of rock thermal conductivity. *Geothermics* **66**, (2017), 1-12.

Ármannsson, H., Fridriksson, T. and Kristjánsson, B.R.: CO_2 emissions from geothermal power plants and natural geothermal activity in Iceland. *Geothermics* **34**, (2005), 286-296.

Bédard, K., Comeau, F.-A., Raymond, J., Malo, M. and Nasr, M.: Geothermal Characterization of the St. Lawrence Lowlands Sedimentary Basin, Québec, Canada. *Natural Resources Research* **27**, (2017), 479-502.

Benson, P.M., Meredith, P.G. and Platzman, E.S.: Relating pore fabric geometry to acoustic and permeability anisotropy in Crab Orchard Sandstone: A laboratory study using magnetic ferrofluid. *Geophysical Research Letters* **30**, (2003).

Brigaud, F. and Vasseur, G.: Mineralogy, porosity and fluid control on thermal conductivity of sedimentary rocks. *Geophysical Journal International* **98**, (1989), 525-542.

Cho, W.J., Kwon, S. and Choi, J.W.: The thermal conductivity for granite with various water contents. *Engineering Geology* **107**, (2009), 167-171.

Chopra, N., Ray, L., Satyanarayanan, M. and Elangovan, R.: Evaluate best-mixing model for estimating thermal conductivity for granitoids from mineralogy: A case study for the granitoids of the Bundelkhand craton, central India. *Geothermics* **75**, (2018), 1-14.

Clauser, C.: Thermal Storage and Transport Properties of Rocks. *Encyclopedia of Solid Earth Geophysics*, (2014), 1431–1440.

Côté, J. and Konrad, J.-M.: Thermal conductivity of base-course materials. *Canadian Geotechnical Journal* **42**, (2005), 61-78.

Di Sipio, E., Chiesa, S., Destro, E., Galgaro, A., Giaretta, A., Gola, G. and Manzella, A.: Rock Thermal Conductivity as Key Parameter for Geothermal Numerical Models. *Energy Procedia* **40**, (2013), 87-94.

Fuchs, S. and Förster, A.: Well-log based prediction of thermal conductivity of sedimentary successions: a case study from the North German Basin. *Geophysical Journal International* **196**, (2014), 291-311.

Fuchs, S., Schütz, F., Förster, H.-J. and Förster, A.: Evaluation of common mixing models for calculating bulk thermal conductivity of sedimentary rocks: Correction charts and new conversion equations. *Geothermics* **47**, (2013), 40-52.

Gehne, S. and Benson, P.M.: Permeability and permeability anisotropy in Crab Orchard sandstone: Experimental insights into spatio-temporal effects. *Tectonophysics* **712-713**, (2017), 589-599.

Guo, P., Bu, M., He, M. and Wang, Y.: Experimental investigation on thermal conductivity of clay-bearing sandstone subjected to different treatment processes: Drying, wetting and drying II. *Geothermics* **88**, (2020).

Hu, J., Cheng, Y., Li, Z., Zhang, Y., Yan, H. and Huang, J.: An integrated approach for thermal conductivity prediction of grotto sandstone using virtual sample generation and machine learning with limited nondestructive testing data. *Measurement* **256**, (2025).

Ibemesi, P. and Benson, P.: Effect of Pressure and Stress Cycles on Fluid Flow in Hydraulically Fractured, Low-Porosity, Anisotropic Sandstone. *Rock Mechanics and Rock Engineering* **56**, (2022), 19-34.

Jorand, R., Clauser, C., Marquart, G. and Renate, P.: Statistically reliable petrophysical properties of potential reservoir rocks for geothermal energy use and their relation to lithostratigraphy and rock composition: The NE Rhenish Massif and the Lower Rhine Embayment (Germany). *Geothermics* **53**, (2015), 413-428.

Jorand, R., Fehr, A., Koch, A. and Clauser, C.: Study of the variation of thermal conductivity with water saturation using nuclear magnetic resonance. *Journal of Geophysical Research* **116**, (2011).

Kagel, A., Bates, D. and Gawell, K.: A guide to geothermal energy and the environment. United States (2005).

Kämmlein, M. and Stollhofen, H.: Pore-fluid-dependent controls of matrix and bulk thermal conductivity of mineralogically heterogeneous sandstones. *Geothermal Energy* **7**, (2019).

Kappelmeyer, o. and Haenel, R.: Geothermics with Special Reference to Application. *Geoexploration Monograph*, (1974).

Kocurek Industries: Details For Crab Orchard. KOCUREK Industries, Inc. - Hard Rock Division,(2023)

Labus, M. and Labus, K.: Thermal conductivity and diffusivity of fine-grained sedimentary rocks. *Journal of Thermal Analysis and Calorimetry* **132**, (2018), 1669-1676.

Mielke, P., Bär, K. and Sass, I.: Determining the relationship of thermal conductivity and compressional wave velocity of common rock types as a basis for reservoir characterization. *Journal of Applied Geophysics* **140**, (2017), 135-144.

Murphy, D.T., Allen, C.M., Ghidan, O., Dickson, A., Hu, W.P., Briggs, E., Holder, P.W. and Armstrong, K.F.: Analysing Sr isotopes in low-Sr samples such as single insects with inductively coupled plasma tandem mass spectrometry using N(2) O as a reaction gas for in-line Rb separation. *Rapid Commun Mass Spectrom* **34**, (2020).

Nagaraju, P. and Roy, S.: Effect of water saturation on rock thermal conductivity measurements. *Tectonophysics* **626**, (2014), 137-143.

Nehler, M., Stoeckhert, F., Oelker, A., Renner, J. and Saenger, E.: Evaluating porosity estimates for sandstones based on X-ray micro-tomographic images. *Solid Earth Discuss* **-**, (2019).

Pichugin, Z., Chekhonin, E., Popov, Y., Kalinina, M., Bayuk, I., Popov, E., Spasennykh, M., Savelev, E., Romushkevich, R. and Rudakovskaya, S.: Weighted geometric mean model for determining thermal conductivity of reservoir rocks: Current problems with applicability and the model modification. *Geothermics* **104**, (2022).

Popov, Y., Beardsmore, G., Clauser, C. and Roy, S.: ISRM Suggested Methods for Determining Thermal Properties of Rocks from Laboratory Tests at Atmospheric Pressure. *Rock Mechanics and Rock Engineering* **49**, (2016), 4179-4207.

Popov, Y.A., Pribnow, D.F.C., Sass, J.H., Williams, C.F. and Burkhardt, H.: Characterization of rock thermal conductivity by high-resolution optical scanning. *Geothermics* **28**, (1999), 253-276.

Raymond, J.: Colloquium 2016: Assessment of subsurface thermal conductivity for geothermal applications. *Canadian Geotechnical Journal* **55**, (2018), 1209-1229.

Raymond, J., Comeau, F., Malo, M., Blessent, D. and López-Sánchez, I.: The Geothermal Open Laboratory: a free sace to measure thermal and hydraulic properties of geological materials. *Conference*, IGCP636 Annual Meeting 2017, Santiago de Chile, Chile (2017).

Rietveld, H.M.: Line profiles of neutron powder-diffraction peaks for structure refinement. *Acta Crystallographica* **22**, (1967), 151-152.

Song, J., Wang, G., Xing, L., Qian, J., Dai, L. and Di, H.: Influencing factors of rock thermal conductivity and applicability evaluation of its mixing law predictive models. *Geothermics* **110**, (2023).

Suft, O., Hagenauer, H. and Bertermann, D.: Relationship Between Thermal Conductivity, Mineral Composition and Major Element Composition in Rocks from Central and South Germany. *Geosciences* **15**, (2025).

Tang, B., Zhu, C., Qiu, N., Cui, Y., Guo, S., Luo, X., Zhang, B., Li, K., Li, W., Fu, X. and Luo, X.: Analyzing and Estimating Thermal Conductivity of Sedimentary Rocks from Mineral Composition and Pore Property. *Geofluids* **2021**, (2021), 1-19.

Tatar, A., Mohammadi, S., Soleymanzadeh, A. and Kord, S.: Predictive mixing law models of rock thermal conductivity: Applicability analysis. *Journal of Petroleum Science and Engineering* **197**, (2021).

Umar, M., Awosusi, A.A., Adegboye, O.R. and Ojekemi, O.S.: Geothermal energy and carbon emissions nexus in leading geothermal-consuming nations: Evidence from nonparametric analysis. *Energy & Environment* **35**, (2023), 2726-2752.

Velcin, H.: Integrated multi-scale petrophysical methods for core characterisation applied to siliciclastic reservoirs. Doctor of Philosophy (The University of Western Australia). 336 p(2022).

Vivas, C., Hu, Z. and Salehi, S.: Texture-Dependent Thermal Properties of Sandstone Rocks Examined by Scanning Electron Microscopy for Thermal Energy Storage Applications. *ASME Open Journal of Engineering* **2**, (2023).

Vroon, P.Z., van der Wagt, B., Koornneef, J.M. and Davies, G.R.: Problems in obtaining precise and accurate Sr isotope analysis from geological materials using laser ablation MC-ICPMS. *Anal Bioanal Chem* **390**, (2008), 465-476.

Williams, S.A. and French, M.E.: Effects of Dilatant Hardening on Fault Stabilization and Structural Development. *Geophysical Research Letters* **51**, (2024).

Wu, H., Liu, Y., Yang, M., Zhang, J. and Zhang, B.: Effect of temperature-dependent rock thermal conductivity and specific heat capacity on heat recovery in an enhanced geothermal system. *Rock Mechanics Bulletin* **2**, (2023).

Ye, X., Yu, Z., Zhang, Y., Kang, J., Wu, S., Yang, T. and Gao, P.: Mineral Composition Impact on the Thermal Conductivity of Granites Based on Geothermal Field Experiments in the Songliao and Gonghe Basins, China. *Minerals* **12**, (2022).